Successful vibration analysis on a 200 MW pump turbine in Luxembourg

Dr.-Ing. Patrick Tetenborg, Dr.-Ing. Johann Lenz, Dipl.-Ing. Gilles Nosbusch

The Vianden pumped-storage power plant in Luxembourg began operating at the end of the fifties and has since been expanded in various stages of construction. It is used to store excess energy – such as wind energy – and also to cover demand peaks. At times when consumption is low, for example at night, the excess energy from the base load power plants is used to pump water from the lower to the upper reservoir (storage). When the demand for electricity increases, the stored water flows through turbines back into the lower reservoir (see Figure 1).

The overall installed turbine capacity is almost 1,300 MW. 1,040 MW is available in the pumping operation. The pumped-storage power plant is divided into a cavern power plant (machines 1 through 9), a shaft power plant (machine 10) and a separate cavern for machine 11 (M11). The cavern power plant encompasses 9 horizontally arranged three-part hydroelectric generating sets, each with a turbine capacity of 100 MW and a pump capacity of 70 MW. The shaft power plant consists of a vertical two-part hydroelectric generating set with a turbine capacity of 196 MW and a pump capacity of 220 MW. In 2010 the power plant was expanded with machine 11, an additional 200 MW pump turbine (see Figure 2). To inaugurate this system at the end of 2014, Joachim Gauck who was then the Federal President of Germany arrived in the course of a state visit to put machine 11 into operation together with the Grand Duke Henri of Luxembourg. The M11 is equipped with a Francis turbine (diameter 4.3 m), custom-made for pumping and turbine operation. It can be operated at a nominal flow rate of 78,200 l/s, turbine capacity of 197 MW and pump capacity of 196 MW.

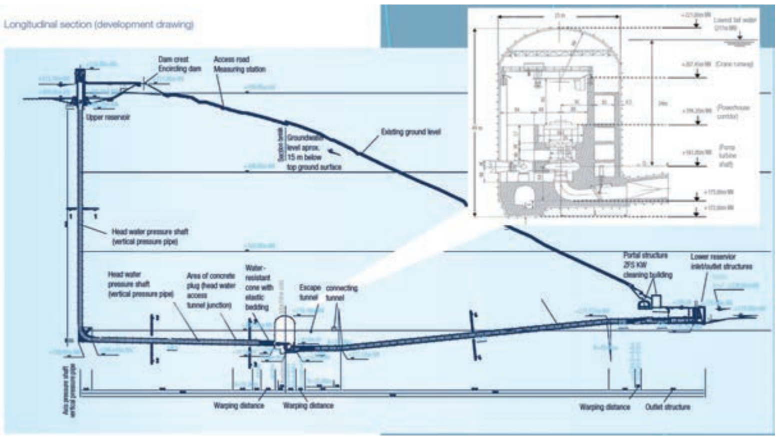

Fig. 2: Sectional drawing showing the arrangement of machine 11 with an enlargement of the underground cavern (source: SEO).

Fig. 1: Aerial photo of the separate upper and lower reservoirs along with the dammed course of the river (Our) in Vianden (Luxembourg).

Initial situation and problem

The distinguishing feature of machine 11 upon commissioning was its extremely quiet operation across a wide operating range, both in pump and in turbine operation. Ever since it was put into operation however, a pronounced 150 Hz vertical vibration has occurred on the pump turbine set in the upper range of performance at approximately 180 MW, and is clearly audible as an individual note in the underground cavern. Several international experts specialising in hydroelectric power plants were consulted to find the cause. The results of measurements were as follows:

1. Due to the otherwise quiet operation and narrow frequency range, the vibrations were relatively noticeable as a low humming sound and very easy to reproduce.
2. The vibrations occurred in a load range of 160 MW to 190 MW during turbine operation.
3. A minor variation in the output at which the vibrations occurred was found depending on the head of water. The phenomenon always occurred at the same volume flow regardless of the head of water.

An inadequate axial offset between the impeller and housing was considered as a possible reason why the vibrations were load-dependent. Changing the load range of the vibrations by changing the axial thrust was therefore attempted. In order to do so, the inside diameter of the flow restrictor inserted in the turbine cover pressure relief pipe (see Figure 3) was reduced. However, the resulting increased axial thrust did not produce any change. The maximum vibrations continued to occur at approximately 180 MW. On the other hand, the oscillation amplitudes and frequency did change, increasing slightly.

As a second measure, the impeller was installed 1 mm lower. This however did not produce the desired result either. In conclusion, the experts confirmed that such a phenomenon has not previously occurred in pump turbines.

Due to the unclear situation, the independent engineering firm specialising in sound and vibration engineering KÖTTER Consulting Engineers GmbH & Co. KG was then consulted for the first time. Regular check measurements (fingerprint measurements) were to be taken to observe the phenomenon and detect characteristic changes in the operating behaviour (for example due to damage) in a timely manner. In addition, a root cause analysis was to be performed independently of the previous expert reports. Several series of measurements were taken for this purpose under various operating conditions. Here the plant output was increased step by step over a period of about 5 minutes while the vibrations and pressure fluctuations were recorded.

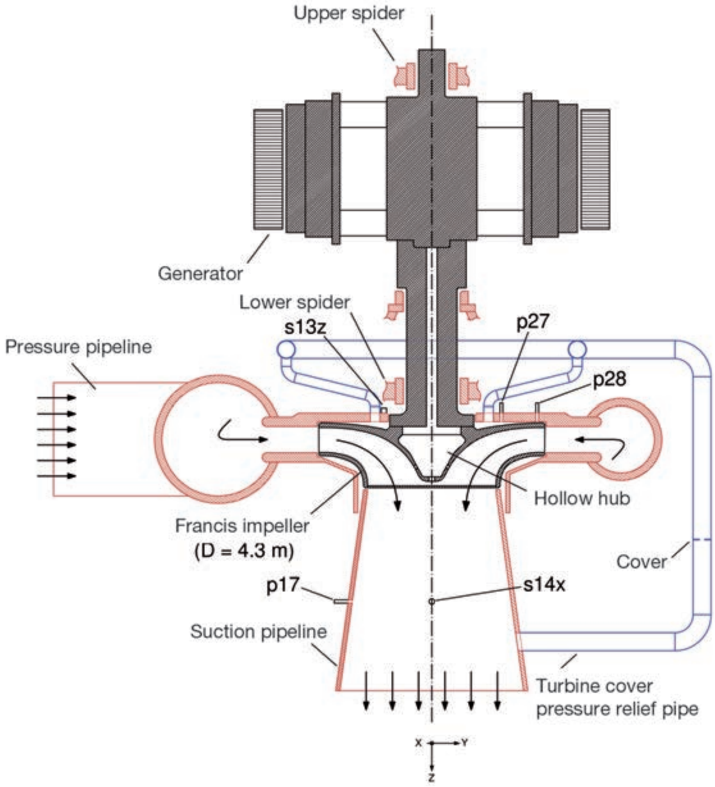

Fig. 3: Schematic diagram of the pump turbine structure with selected vibration measuring points (s13z, s14x) and pressure measuring points (p17, p27, p28).

Metrological investigation

Figure 4 presents an excerpt of the recorded vibrations as effective values and peak-to-peak values of the measured pressure fluctuations while changing the plant output step by

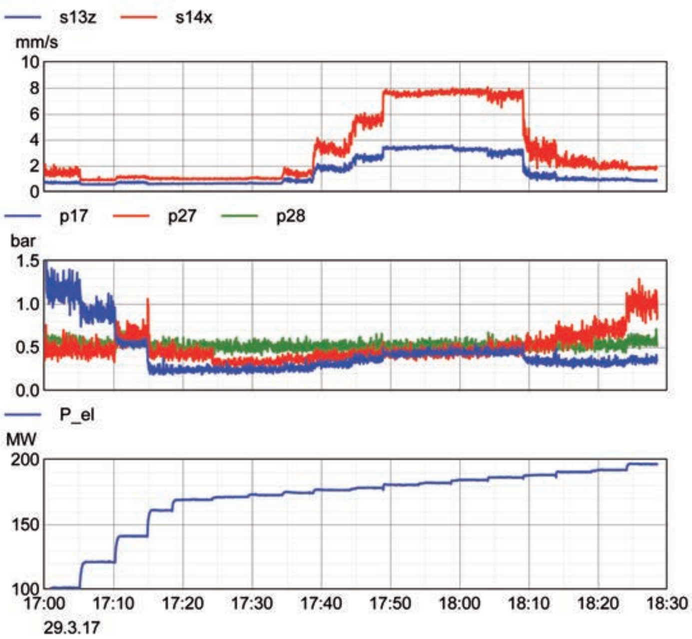

Fig. 4: Measured effective vibration speeds and peak-to-peak values on the intake pipe cone and turbine cover with corresponding output curve in turbine operation.

step over time. The effective vibration speed curves show an increase in the vibration level starting at approximately 174 MW, both on the turbine cover (s13z) and on the intake pipe cone (s14x). The maximum effective values are at approximately 180–184 MW. For the pressure fluctuations, the behaviour is not as clear. While the fluctuations on the intake pipe cone (p17) show tendencies similar to the vibration speeds, no correlation was initially detectable in the area of the turbine cover (p27 and p28). This is due among other things to the implementation of the pressure measuring points on the turbine cover. There is no way of venting them and their usefulness for the root cause analysis is generally limited.

Thus, the phenomenon occurred both below (pressure fluctuations in the intake pipe cone and surface vibrations of the intake pipe cone) and above (vibrations of the turbine cover) the pump turbine. This finding as well as the investigations previously conducted by experts indicated an influence of the turbine cover pressure relief pipe. It connects the intake pipe to the upper lateral chamber of the impeller in order to ensure adequate axial thrust equalisation. Acoustic resonance effects constitute a possible influencing mechanism.

Acoustic simulation

Direct metrological recording of the pressure fluctuations within the turbine cover pressure relief pipe was not possible at this time. In order to make a statement about its possible influence regardless, the pressure fluctuations of the turbine cover pressure relief pipe were simulated in a subsequent step.

Figure 6 presents an excerpt of the modelled turbine cover pressure relief pipe and a one-dimensional illustration of the circular ring of the lateral impeller chamber. The investigated excitation positions and the positions of nodes relevant for the results are shown as well. A schematic of the evaluation is also presented. The simulations were performed in the time domain. The acoustic model was continuously excited using a frequency

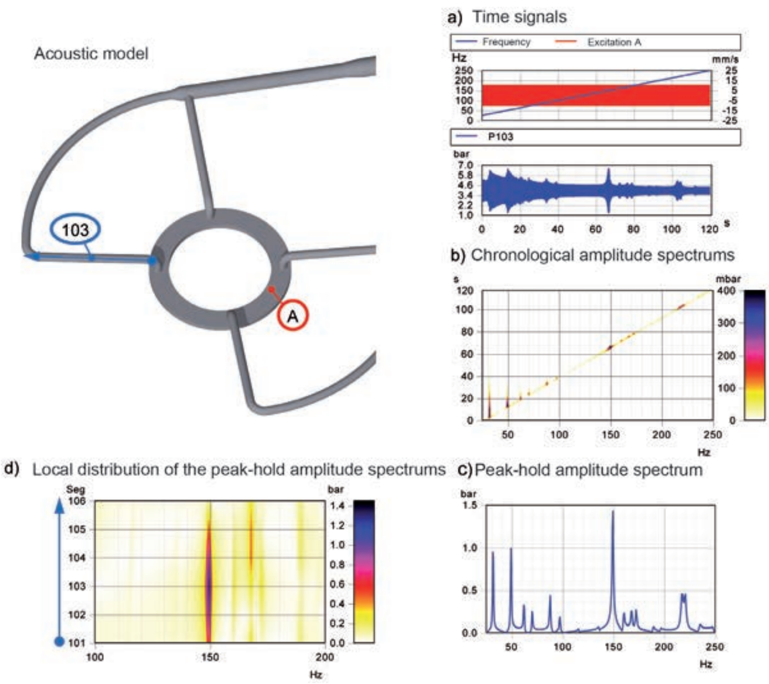

Fig. 5: Exemplary illustration of the calculation results: Pressure fluctuations at node 103 as time signal, as colour chart illustration with chronological amplitude spectrums, as peak-hold amplitude spectrum of the individual spectrums, and as local distribution of the peak-hold amplitude spectrum in a colour chart.

ramp. Amplitude spectrums were used to evaluate the local response of the system. In order to subsequently analyse the transmission behaviour, location and frequency-dependent colour charts were used in conclusion.

In a first calculation step, the model was used to determine the acoustic transmission behaviour in the pipe as the actual situation. For this purpose, various exciter positions (here as an example: A) were used to induce pressure fluctuations in the lateral impeller chamber by specifying a frequency sweep of 25 to 250 Hz with a constant sound particle velocity amplitude. The system's acoustic transmission behaviour leads to different local distributions of the fluctuations depending on the excitation frequency and position. An acoustic resonance at approximately 150 Hz within the turbine cover pressure relief pipe was indicated by the simulation results.

But since local measurement results were not available and a distinct excitation mechanism could not be identified either, the acoustics of the turbine cover pressure relief pipe were temporarily altered. If acoustic resonance was responsible for the 150 Hz vibration phenomenon, this measure would cause a considerable change in the operating behaviour. By simply closing two of the four arms of the turbine cover pressure relief pipe in an on-site test, it was determined that the acoustics within the turbine cover pressure relief pipe did not play a crucial role for the vibration phenomenon.

Comprehensive analysis

Since this approach did not yield results, the existing materials and measurement results were once again intensively reviewed and analysed. The following causes could already be excluded based on the existing findings:

– Generator-induced vibrations
– Improper impeller alignment
– Axial thrust influences
– Excitation by harmonics of the rotation noise
– Acoustic amplification by the turbine cover pressure relief pipe

The implementation of measuring points p27 and p28 came into focus again during the repeat analysis.

While the pressure signals had already been included in the recordings of the previous experts, they were not used further for the analysis due to the lack of venting. Figure 6 presents a detailed view showing the exact location and implementation of measuring point p27. The air in the connection bore cannot escape when the system is flooded. An air cushion therefore forms directly below the sensor head. This results in a system capable of vibration that, similar to a spring-mass system, is defined by the compressibility of the air (equivalent to stiffness) and the inertness of the water mass.

ginally transmitted to the measuring point, and that the air-water column acts as a low-pass filter.

By using the analogy of this air-water column that is capable of vibration and a spring-mass system, the transmission of the local fluctuations can be estimated using an enlargement function for a spring-mass system. For supercritical excitation, this is significantly influenced by the frequency ratio. Assuming a resonance frequency of this air-water column of about 25 Hz, a frequency ratio of $\eta = 6$ results in the following amplification factor V for the transmitted pressure fluctuations:

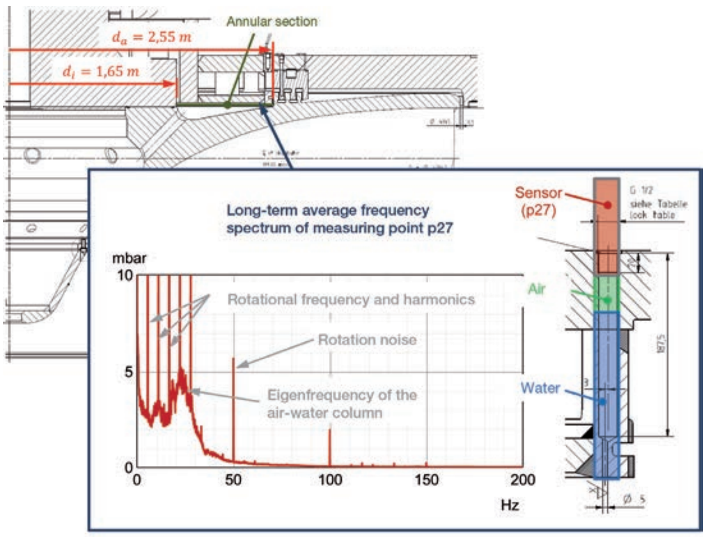

Fig. 6: Detail showing the location and implementation of measuring point p27 with a long-term average frequency spectrum at a turbine output of 160 MW.

For a qualitative determination of the transmission behaviour of the pressure fluctuations in the lateral impeller chambers at the measuring points, a noise band can be determined via long-term frequency spectrums (see Figure 6). In examining a noise band, it is assumed that all frequencies are stochastically excited by the turbulent flows so that a qualitative transmission behaviour can be determined. Averaging the spectrum at a very high resolution makes it possible to approximate the resonance frequency of the air-water column. This spectrum shows that high-frequency fluctuations in the area close to the hub of the lateral impeller chamber are only mar-

$$V = f\left(\eta = \frac{150\ Hz}{25\ Hz} = 6\right) = \frac{1}{\sqrt{(1-\eta^2)^2}} = 0{,}029$$

According to this theory, the actual pressure fluctuations in the lateral impeller chamber were greater than the pressure fluctuations recorded at the measuring point, by a factor of 35 (reciprocal value of 0.029).

Based on this finding, the correlation of the pressure fluctuations at measuring point p27 were compared again to the vibrations on the turbine cover s13z and on the intake pipe s14z (see Figure 7). The curves show a very good quantitative correlation. The signals are proportional up to the vibration maximum and show slight devia-

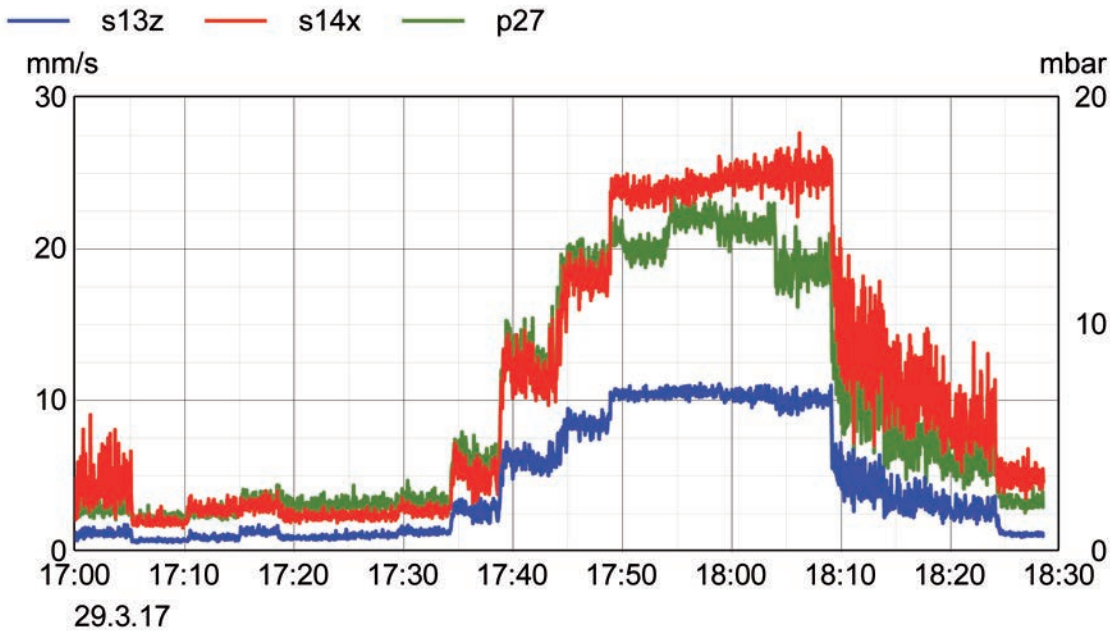

Fig. 7: Qualitative comparison of the bandpass-filtered peak-to-peak vibration velocities from 140 Hz to 160 Hz and the fluctuations at measuring points s13z, s14x and p27.

tions in the trend only at the vibration maximum.

In order to estimate the possible relevance of these local pressure fluctuations for the 150 Hz vibration phenomenon, the local pressure fluctuations were converted to an equivalent axial force. A homogeneous pressure distribution in the lateral impeller chamber close to the hub was assumed for this purpose. Under consideration of the corresponding annular section (see Figure 6), the corresponding axial force that is transferred to the turbine cover and the impeller can be calculated:

$$F_{ptop} = p_{ptop} \cdot \frac{1}{V(\eta = 6)} \cdot \frac{\pi}{4} \cdot \left(d_a{}^2 - d_i{}^2\right)$$
$$= 166\ kN$$

Based on the magnitude, the local pressure fluctuations constituted a possible excitation mechanism for the 150 Hz vibration phenomenon. The position of the force excitation also explained why the turbine cover vibrations at measuring point s13z in particular increased sharply.

Furthermore, the transmission of the local fluctuations through the diagonal equalisation bores in the cavity of the hub and through the adjacent equalisation bores into the flow channel itself was also conceivable. This could also explain the increased vibration level on the intake pipe cone and the pronounced fluctuations in the intake pipe cone.

After high pressure fluctuations were identified as a plausible excitation mechanism for the recorded vibration level, the cause of these pressure fluctuations had to be analysed in greater detail. Flow-induced vortex shedding was a possible excitation mechanism. This could for example occur on the eight bores to the flow channel or in the area of the labyrinth seal in the vicinity of measuring point p27 (see Figure 6). Further information about the flows through and around the bores was required from the manufacturer in order to assess this possibility.

A detailed examination of the fundamental character of the 150 Hz vibration showed that the vibration phenomenon only occurred in a very narrow-band range (see Figure 8). Furthermore, the vibration frequency at measuring point s13z appeared to remain at a fixed frequency of approximately 149 Hz here, even when the output was continuously increased via the volume flow. Such a latching is often explained by the involvement of structural-mechanical or acoustic resonance effects. An acoustic resonance in the hub cavity due to excitation by vortex shedding could therefore constitute a plausible mechanism causing the 150 Hz vibration phenomenon.

Strike tests were performed with the drained pump turbine to characterise the structural-mechanical properties of the impeller. A weakly damped distinctive impeller

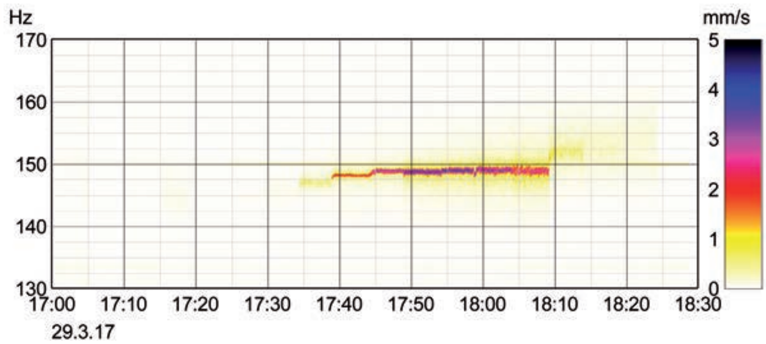

Fig. 8: Chronological sequence of amplitude spectrums for the vibration velocities on the turbine cover (s13z) as colour charts.

eigenmode at 150 Hz was determined in the process. The transferability of the results to the structural-dynamic properties with surrounding water is generally limited. However, the weak damping and good correlation indicated an involvement with the vibration phenomenon.

However, the structural eigenmode of the impeller at approximately 150 Hz exhibited a nearly linear damped vibration behaviour. In linear systems capable of vibration with adequate damping ratios, a continuous broadband increase of one vibration component is expected. The very narrow-band occurrence of the increased fluctuations or vibrations seen here is typical among other things for Helmholtz resonators.

The area of the hub cavity and the annual space below the annual section at measuring point p27 (Figure 6, top) constitute an acoustic system similar to a Helmholtz resonator. In order to pragmatically assess the possibility of amplification occurring in this area, the eigenfrequency for an equidistant Helmholtz resonator was approximated. An initial assumption was made on the basis that the central hub cavity constitutes the volume and the discharge bores towards the flow channel constitute the inductive bottlenecks. The resonator frequency estimated using this approach is 121 Hz.

Alleviation measure

Altering the acoustics of the hub region would be a possible approach to eliminating the problem. Implementing such a measure by geometrical modifications is however costly and associated with comparatively long downtime.

A modification of the fluid properties – in particular the acoustic velocity – that could be implemented quickly was preferred over a geometric modification. Air injection tests – as close to the hub as possible – with a significant influence on the resonator were deemed suitable for implementation.

These tests were completed in a timely manner (also see Figure 9). The operating point with the 150 Hz vibration component was specifically chosen here. Then air was injected at various intervals for approximately 5 seconds at the original measuring point p27. The influence was visible in the pressure fluctuations, both in the intake pipe cone and on the turbine cover. The 150 Hz components abruptly disappeared at the time of air injection. Remaining, residual fluctuations and residual vibrations in the effective value curves are due to behaviour that is typical for the system (rotation noise, flow turbulences etc.).

The injection of air reduced the sound velocity of the water-air mixture from approximately 1,400 m/s for pure water to a fraction of this value. This drop was due to the ratio between the compressibility and density of a fluid that is relevant for the sound velocity. While the density remained approximately the same, the injected air considerably increased the compressibility of the medium. Thus, the medium is now easier to compress, resulting in a lower sound wave propagation velocity. This shifts the acoustic resonance frequency downward almost proportionally to the sound velocity so that dominant excitation is stopped.

After most of the air had been transported away, the compressibility decreased continuously. The sound velocity of the mixture changed again to the sound velocity of pure water. The sound velocity is highly dependent on the presence of air at a low per cent by volume (< 0.1 %). This dependency explains the very steep increase in the vibration frequency of the humming component from approximately 135 to 145 Hz. As previously mentioned, this increase is due to the dependency of the acous-

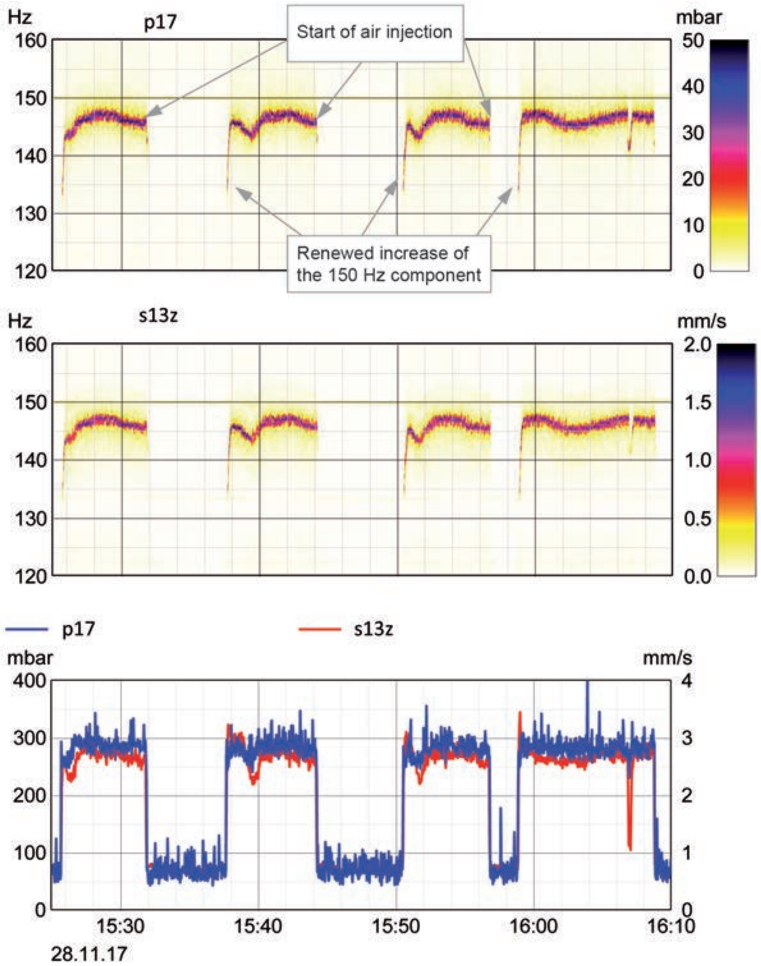

Fig. 9: Colour spectrums of measuring points p17 and s13z as well as the corresponding peak-to-peak curve for measuring point p17 and effective value curve for measuring point s13z.

tic resonance frequency on the sound velocity. When there was no more air in the area of the hub cavity, the vibration frequency once again stabilised slightly below 150 Hz.

Conclusion

After numerous extensive investigations by various international experts, the engineering firm successfully determined the causative mechanism responsible for the 150 Hz vibration phenomenon occurring on machine 11 in the Vianden pumped-storage power plant since it was put into operation in 2014. The alleviation measure that was implemented in the short run, which significantly alters the acoustic transmission behaviour in the relevant hub area through the injection of air, entirely eliminates the 150 Hz vibration phenomenon. Final clarification of the economic and energy efficiency effects of this measure by the operating company and manufacturer is still required. A final geometric modification of the hub region may still be performed depending on those effects. The fundamental approach to solving the problem – altering the acoustic transmission behaviour in the hub region – remains unchanged in any case.

The Authors:
Dr.-Ing. Patrick Tetenborg
Project Engineer
KÖTTER Consulting Engineers GmbH & Co. KG, Rheine, Germany
Dr.-Ing. Johann Lenz
Managing Director
KÖTTER Consulting Engineers GmbH & Co. KG, Rheine, Germany
Dipl.-Ing. Gilles Nosbusch,
Chef de Service adjoint
SEO S.A. Centrale de Vianden, Stolzembourg, Luxembourg